FLAC Simulation of Split-Pipe Tests on an Instrumented Cable Bolt

Marc Ruest
Itasca Consulting Group, Inc., Minneapolis, MN, USA

Lewis Martin
Spokane Research Laboratory, National Institute for Occupational Safety and Health
Spokane, WA, USA

ABSTRACT

A new instrumented cable bolt has been developed by the National Institute for Occupational Safety and Health at the Spokane Research Laboratory in Spokane, WA. Although various instruments are available to measure load distribution and magnitude along a grouted cable, this instrument is innovative in that it uses strain gauges internal to the cable as load-measuring sensors. The instrument has been successfully tested in the field at FMC's Granger Mine, Meikle Mine, and Getchell Mine.

A "split-pipe" laboratory pull test was performed on each of three cable bolts instrumented with the new device. Each test consisted of grouting a 1.83-m-long cable in two 0.91-m-long sections of schedule 80 pipe. A numerical analysis was then performed in which laboratory boundary conditions were simulated and model properties derived from textbook guidelines. The loads calculated by the model were then compared to the measured loads.

INTRODUCTION

Researchers have conducted a large number of experiments on cable bolts to determine their load characteristics for different grout types, grout ratios, and cable configurations (Garford bulb, buttons, birdcage, nut cage, etc.). However, published data are limited on studies of instrumented cables that would provide additional information on loading mechanics (Hyett and Bawden 1997; Choquet and Miller 1987; Goris et al. 1993; Chekired et al. 1997).

The Tensmeg and the SMART cable are two commercially available instruments used to interpret load along a cable bolt. The Tensmeg sensor is a 60-cm-long, externally mounted strain gauge. Multiple Tensmegs are fixed along the cable length to obtain the cable loads at those locations. In the SMART cable, the king wire is replaced by an extensometer with internal wires anchored along the cable and attached to potentiometers within the electrical head. The difference in displacements between anchors is used to calculate average strain, which is then related to load by cable stiffness.

This study presents the results of "split-pipe" tests conducted on a new instrumented cable bolt developed at the Spokane Research Laboratory (SRL). The sensors for this instrument are positioned along the length of a king wire that replaces the steel king wire inside a regular seven-strand cable. The replacement king wire is a strip of steel having strain gauges attached along its length and remolded to a cylindrical shape with epoxy (patent 6,311,564) (Fig. 1).

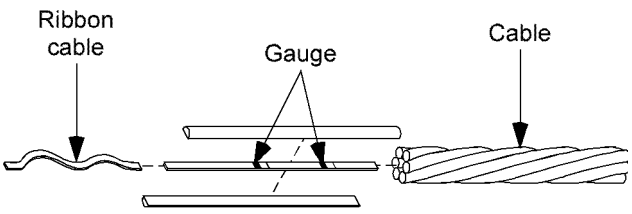

Figure 1.—Instrumented king wire with gauges and connecting cable.

The main advantage of the SRL instrument is that cable stretch is measured over a short distance and can therefore provide an accurate estimate of load over a small (approximately 13 mm) length of cable. Because of their low cost, many strain gauges can be installed along the cable to get a better understanding of load distribution.

EXPERIMENTAL SET-UP AND METHODOLOGY

Three split-pipe tests were conducted. The split-pipe assembly simulates the opening of a crack in a supported rock mass. An instrumented cable with 20 equally spaced gauges was grouted within each pipe assembly (Fig. 2). During the simulation, two 0.91-m-long pipes were pulled apart using a hydraulic load frame, and the reaction loads and pipe displacements were monitored. As the pipes were displaced, the grout transferred axial load to the cable and the strain gauges fixed inside the king wire gave a microstrain reading to a data acquisition system. The data provided a measured load profile along the instrument for a given pipe displacement and resulting reaction load.

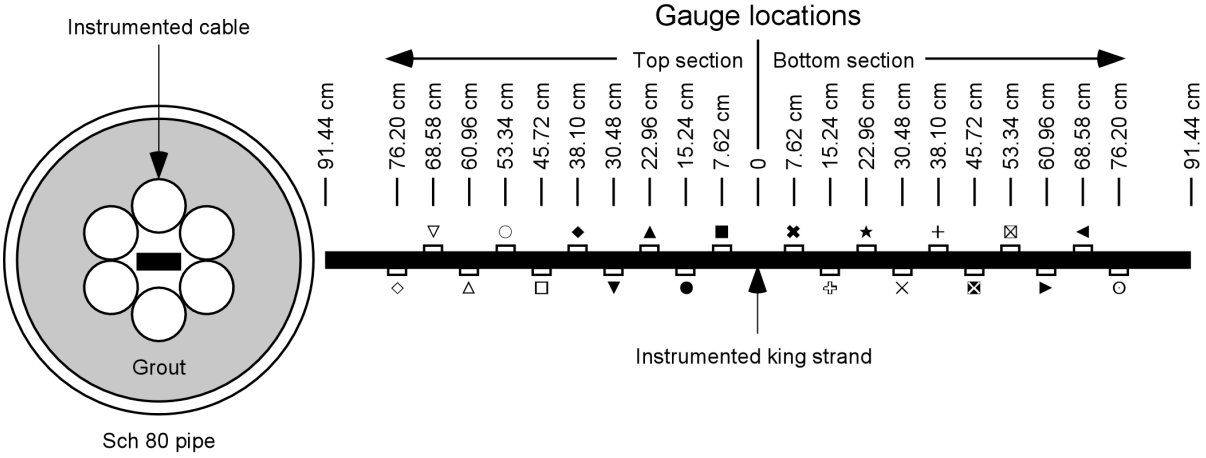

Figure 2.—Instrumented cable grouted in steel pipe.

TEST SET-UP

The first instrumented split-pipe test was conducted 28 days after pouring the sample, and the second and third tests were conducted at 30 days. The mixing ratio of 0.35 water to Type I/II portland cement was used for the grout, achieving an average compressive strength of 57 MPa at 28 days. The instrumented cables were constructed using 15.8-mm diameter, seven-strand conventional cables with breaking strengths of approximately 258 kN. Conventional cables were chosen due to the large database of experimental results available for this cable type. The tests were run on all three samples until the cable slipped and the cable-grout system could no longer hold the loads.

The pull-test apparatus was built to prevent the tubes from twisting during the tests. The test apparatus was one used by Goris during his testing program at the Bureau of Mines (Fig. 3). Centralizing fixtures were welded to the pipe at each end and in the middle, but were not attached to the bolt. End caps with holes were placed on the bottom ends of the pipes while grout was poured into the tubes. A vibrator was attached to the pipes, and a tamping rod was used during pouring to rid the system of entrapped air. A bead welded to the inside of the pipes prevented slippage at the grout-pipe interface (Goris and Conway 1987).

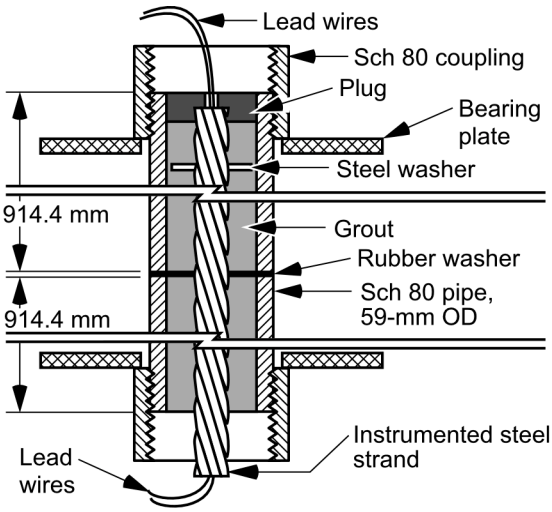

Figure 3.—Pull-test apparatus

CALIBRATION

Tensile tests are used to determine a cable's characteristic load-versus-strain curve. The slope of the elastic portion of the curve is referred to as "cable stiffness," which is required to convert microstrain readings from the gauges in the instrument to a load measurement. The average cable stiffness for the six-strand SRL cable was calculated to be 23,370 kN/m/m. This compares to a stiffness of 28,000 kN/m/m for a standard seven-strand cable. The reduced stiffness was due to the absence of a load-bearing steel king wire.

SPLIT-PIPE TEST RESULTS

The strain measured by the strain gauges is related to the load in the cable bolt by the stiffness determined from the calibration. The results from the laboratory experiment are provided in terms of measured strain at 7.6-cm intervals along the length of the cable versus applied load to the cable. A plot of applied load-versus-measured microstrain for the first experiment is shown in Figure 4. It is convenient to compare load measured on the instrumented cable and load calculated by *FLAC* for increments of applied load. For the purpose of this analysis, the laboratory-measured and *FLAC*-calculated loads are compared for applied loads at 22.2-kN increments. Because the experiment was symmetrical on both sides of the split, we can assume that the gauges measured identical loads at identical distances away from the split. It is therefore valid to average the load measured on both sides for each of the three tests. In total, six data series for load-versus-applied load were averaged to provide one "idealized" data set to compare to the *FLAC* results (Fig. 5).

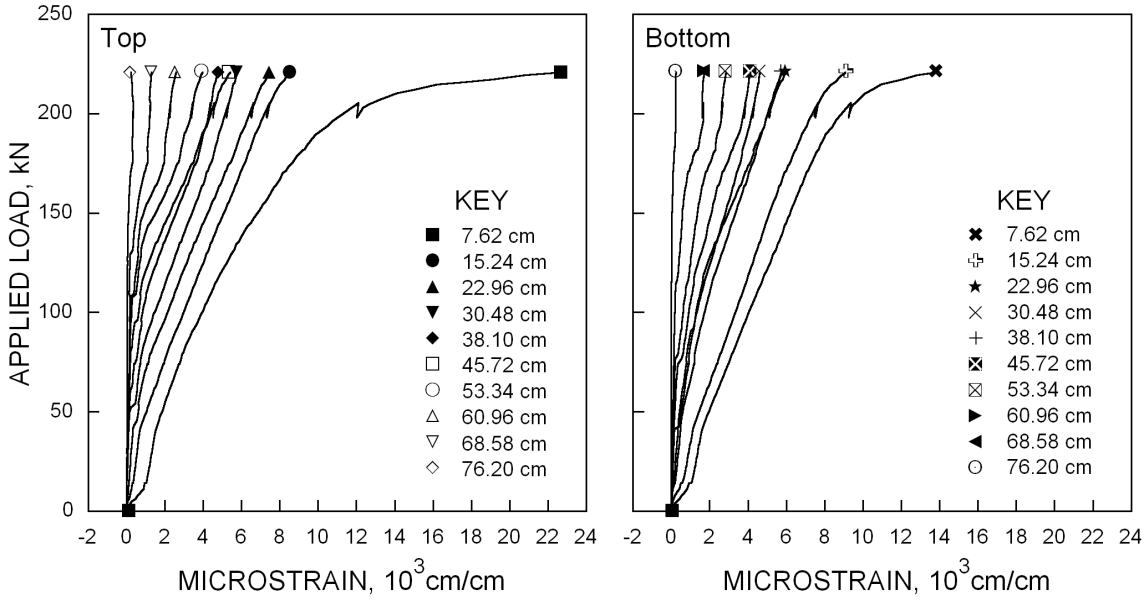

Figure 4.—Pull-test 1.

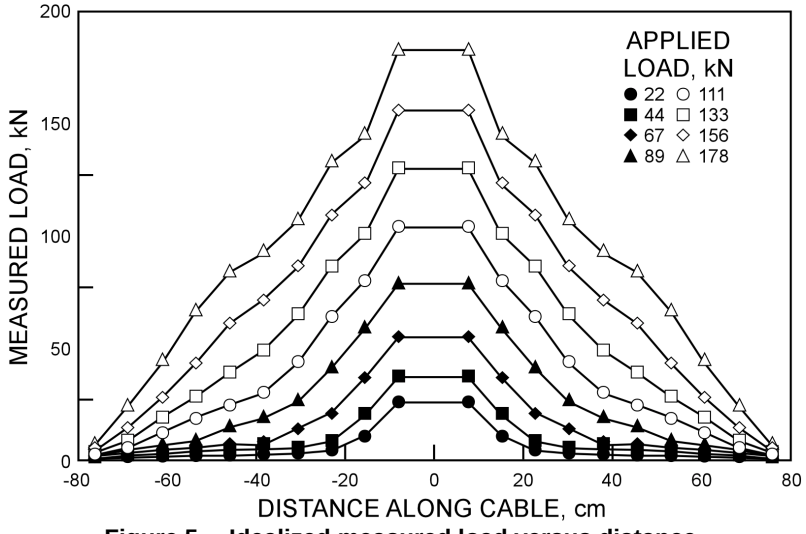

Figure 5.—Idealized measured load versus distance.

MODEL BOUNDARY CONDITIONS AND MATERIAL PROPERTIES

The geometry and boundary conditions for the *FLAC* model are illustrated in Figure 6. In the model, the cable is represented as a series of elements attached at nodes and the split pipe is represented by two rows of zones. The grout bonding the cable to the pipe is implicit in the cable bolt logic. To simulate the pulling apart of the split pipe, a velocity boundary was applied to both ends of the model. This is analogous to pulling each end of the pipe at a constant rate in the laboratory. The two rows of zones are "split" at the model's center by detaching the gridpoints so that both ends of the pipe are free to separate without lateral constraint.

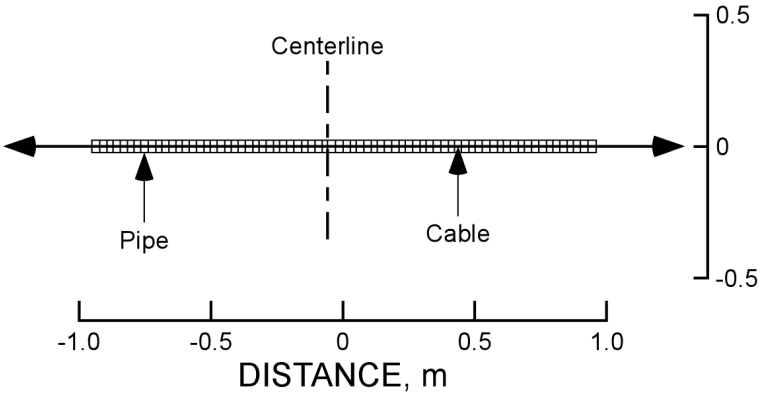

Figure 6.—FLAC model and boundary conditions.

The behavior of the *FLAC* cable element is a function of the steel's behavior (axial behavior) and the behavior of the grout-steel interface (shear behavior). Because it is slender, the cable element does not offer any resistance to bending. The axial behavior of the steel is described by a simple linear relationship between applied strain and resulting force. The cable can theoretically take load in either compression or in tension, but in the following analysis, only the tensile behavior is relevant. Figure 7 schematically illustrates cable axial behavior. The required properties for the cable are its tensile strength, Young's modulus, and cross-sectional area (labeled "yield," "E area," and "ycomp" in the figure, respectively). The assumed dimensions and properties for the cable are summarized in Table 1. For the purpose of this experiment, the yield strength is not relevant since the applied load was kept below the yield strength of the cable.

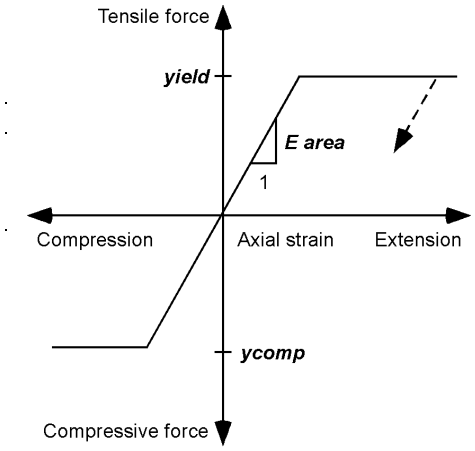

Figure 7.—Axial behavior of FLAC cable element (adapted from Itasca 2000).

TABLE 1.—Cable properties

Property	Model input
Area	$1.826e^{-4}$ m^2
Young's modulus	128 GPa
Yield	220 kN

Shear behavior plays an important role in how the cable is loaded when the grid is displaced. It is through the grout-cable interface that grid displacement induces load in the cable via shear stresses. The shear behavior of the grout is represented as a spring-slider system at the cable nodes (Fig. 8). The properties that describe the grout with reference to Figure 9 are its bond stiffness (**kbond**) and its shear strength (**sbond**). Bond stiffness determines the load applied to the cable through the grout as a result of shear displacement between the grout and the cable. It is usually calculated from field pull-out tests, but such data are not available for the current laboratory setup. The *FLAC* manual provides the following guideline for choosing **kbond** (Itasca 2000).

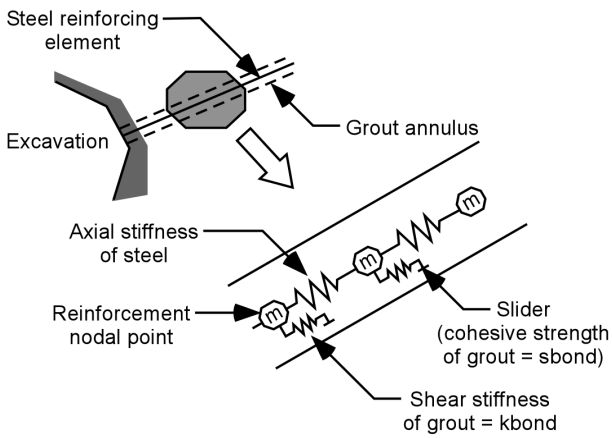

Figure 8.—Conceptual illustration of fully bonded reinforcement (adapted from Itasca 2000).

$$kbond \approx \frac{2\pi G}{10\ln(1+2t/D)} \qquad \text{Eq. 1}$$

In this equation, G is the shear modulus of the grout, t is the radial distance between the cable and the pipe wall, and D is the inside pipe diameter. Therefore, for this split-pipe model and the shear modulus of 0.35 w:c grout (calculated from upper and lower bounds of Young's modulus obtained from Hutchinson and Diederichs [1996] and a Poisson's ratio of 0.20), the starting value for **kbond** is bounded by 6e9 and 8e9 N/m/m. In previous numerical analyses by the senior author, **kbond** was determined from the results of pull tests performed at Complexe Bousquet in Quebec (Ruest 1998). **kbond** was found there to be closer to 3.5e8 N/m/m, one order of magnitude lower than calculated using the equation

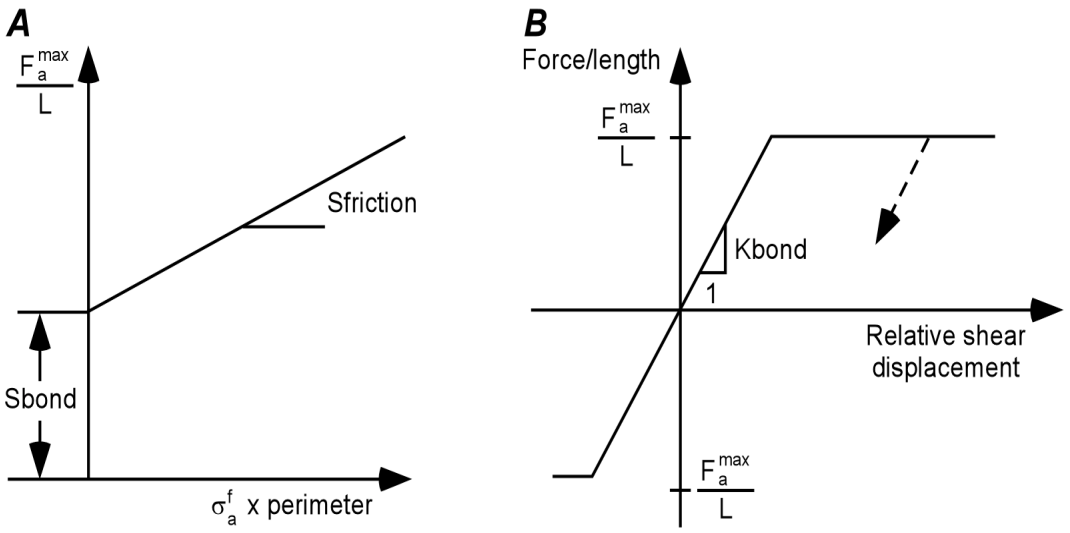

Figure 9.—Grout material behavior for cable elements (adapted from Itasca 2000). *A*, Grout shear strength criterion; *B*, grout shear force versus displacement.

above. In this analysis, the importance of **kbond** was assessed by evaluating the cable's response in the range of 1e8 to 1e10 N/m/m.

Shear strength determines the maximum shear stress in the grout before it begins to slip. Hutchinson and Diederichs have published values for maximum shear stress (referred to as bond strength) as a function of the Young's modulus of the host rock. An equivalent rock modulus for the experimental pipe assembly is found using the following equation (Hutchinson and Diederichs 1996).

$$\frac{E_r}{(1+\nu_R)d_{BH}} = \frac{2E_p(d_o^{\,2} - d_i^{\,2})}{d_i(1+\nu_p)\left\{(1-2\nu_p)d_i^{\,2} + d_o^{\,2}\right\}} \qquad \text{Eq. 2}$$

where E_r = rock modulus,
ν_R = rock Poisson's ratio,
d_{BH} = borehole diameter,
E_P = pipe modulus,
ν_P = pipe Poisson's ratio,
d_i = pipe inside diameter,
and d_o = pipe outside diameter.

With the equivalent rock modulus, the value for **sbond** is determined from the plot of rock modulus versus ultimate bond strength in Figure 10 (taken as **sbond**), also provided by Hutchinson and Diederichs (1996).

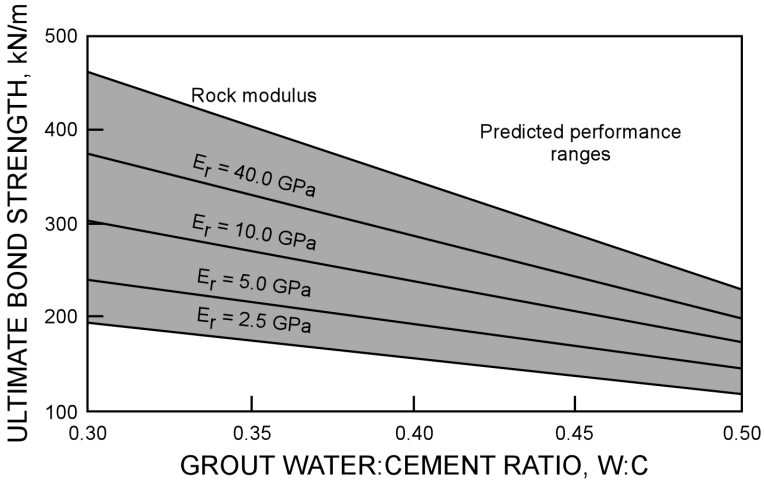

Figure 10.—Ultimate bond strength (in kN/m) as a function of grout quality and rock modulus at 40 mm of slip (Hutchinson and Diederichs 1996). The value of kbond is 1e8 to 1e10 N/m/m, and the value of sbond is 180 to 210 kN/m/m.

It is well known that increases and decreases in confinement will influence cable bolt behavior. *FLAC* attempts to account for this effect by relating confinement on the bolt to maximum shear strength. Increases in confinement are followed by increases in shear strength of the grout, according to the strength criterion defined by the parameter **sfriction** and the grouted perimeter (**perimeter**). In the calibration presented below, no confinement on the cable was modeled (since no confinement was applied to the pipe in the laboratory experiment), and therefore these parameters are irrelevant to the final solution. Thus,

only bond stiffness and grout shear strength were varied. The value of kbond is 1e8 to 1e10 N/m /m, and the value of sbond is 180 to 210 kN/m/m.

MODEL RESULTS

Once the model was constructed and the boundary conditions applied, the reaction forces at the modeled pipe ends were monitored as the two sides were pulled apart. Once the applied load reached one of the 22-kN increments, the load on the cable at 7.6-cm intervals was recorded. The plot in Figure 11shows cable load distribution as calculated by *FLAC* for an applied load of 22 kN. The plot shows how the maximum load is located at the pipe split and that the distribution is symmetrical about the model center. Figure 12 is a plot of the shear force at the grout-cable interface. Because the pipe is displaced in both directions, shear forces are negative on the right-hand side of the split, and equal but opposite in sign on the left-hand side.

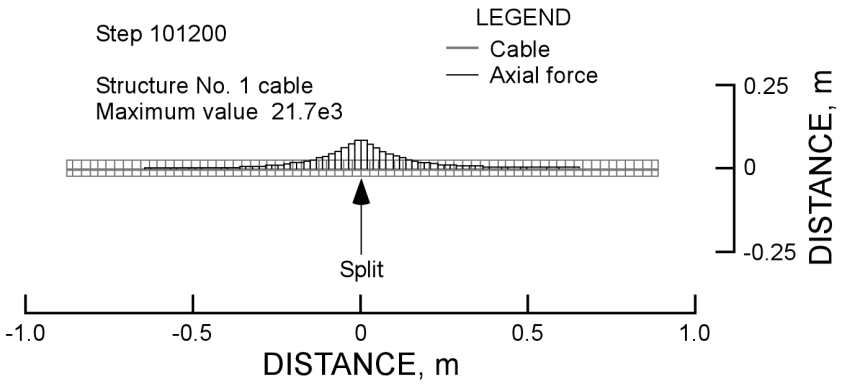

Figure 11.—Plot of load distribution in cable at applied load of 22 kN.

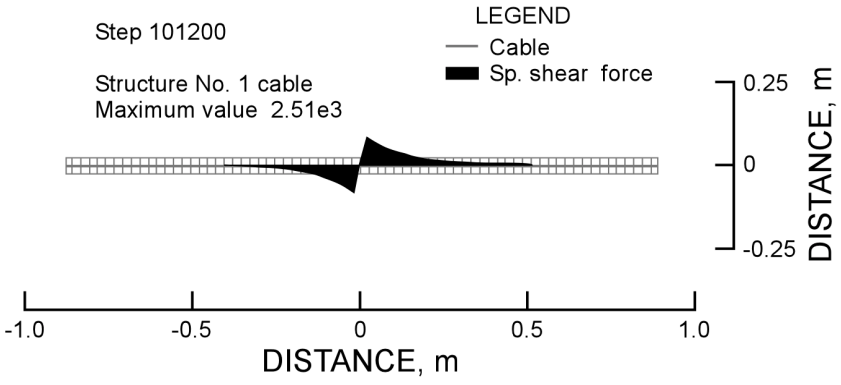

Figure 12.—Plot of shear force at grout-cable interface.

Parametric Analysis of kbond and sbond

Figure 13 shows a plot of the averaged laboratory results and the *FLAC* calculated cable loads for 44- and 117-kN load increments for **kbond** values of 1e8, 1e9, and 1e10 N/m/m. The plot indicates that the shape of the *FLAC* cable curves is very similar to the shape of the idealized laboratory curves for each of the **kbond** values tested, with the lowest stiffness apparently providing the best match for the laboratory results. High loads were observed at the split and decreased with distance from the split. The magnitude of the load at the cable split must be equal to the applied load, but this is not reflected in the plotted data since the load is an average across the element. In each case, the model underpredicts the load in the cable at 7.6 cm (near the pipe center). Improvement diminishes with changes in stiffness. The conclusion from this analysis is that although a reasonable estimate of cable load distribution can be obtained using the previously published equation for **kbond**, a better estimate is obtained using

$$kbond \approx \frac{2\pi G}{100 \ln(1 + 2t / D)} \qquad \text{Eq. 3}$$

Figure 14 shows a plot of load distributions for the model cable at applied loads of 44 and 117 kN for **sbond** values of 180, 190, and 200 kN/m. These values are within the range estimated using Hutchinson and Diederichs ultimate bond strength plot (Fig. 10). There is only a small amount of variability in the model results within the range. Note, however, that the ultimate pull-out load will depend on this parameter. For the model cable to sustain a load of 178 kN as in the laboratory, a minimum **sbond** of 200 kN/m is required.

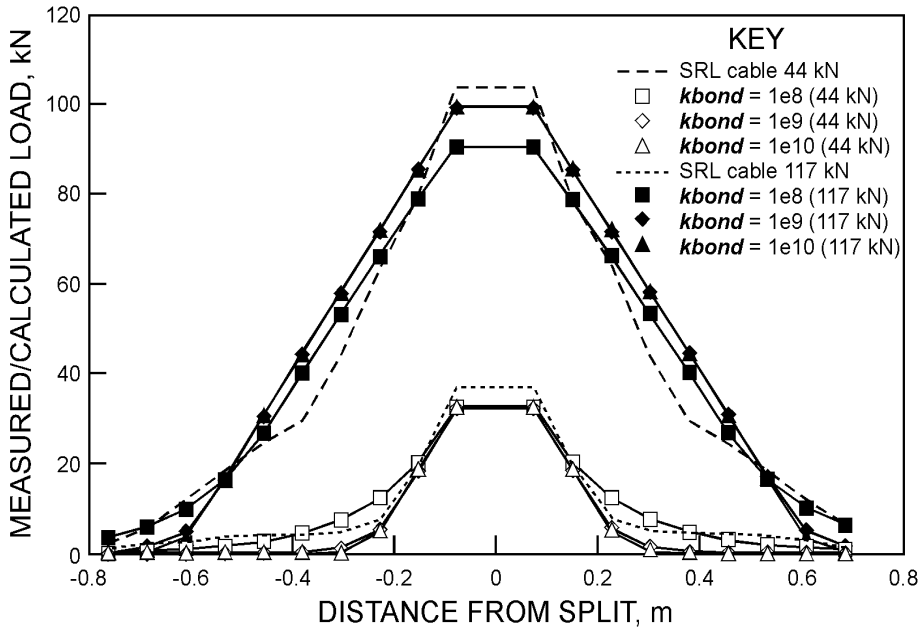

Figure 13.—Load distribution at applied loads of 44 and 117 kN for kbond values of 1e8, 1e9, and 1e10 N/m•m.

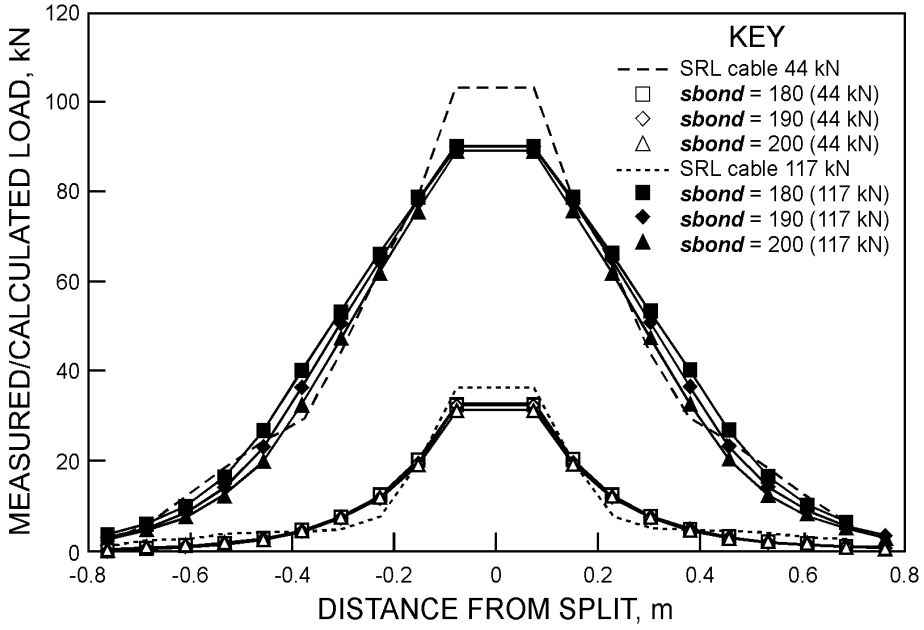

Figure 14.—Load distribution at applied loads of 44 and 117 kN for sbond values of 180, 190, and 200 kN/m.

Final Calibration

Figure 15 provides a plot of the *FLAC*-calculated cable loads compared to the laboratory-determined load distributions for applied loads of 44, 89, 133, and 178 kN. The **kbond** and **sbond** values used to obtain these results were 1e8 N/m/m and 200 kN/m, respectively, as determined from the parametric analysis above. The plot shows that there is very good agreement between the laboratory loads and the loads predicted by *FLAC*. The load at the split is underpredicted

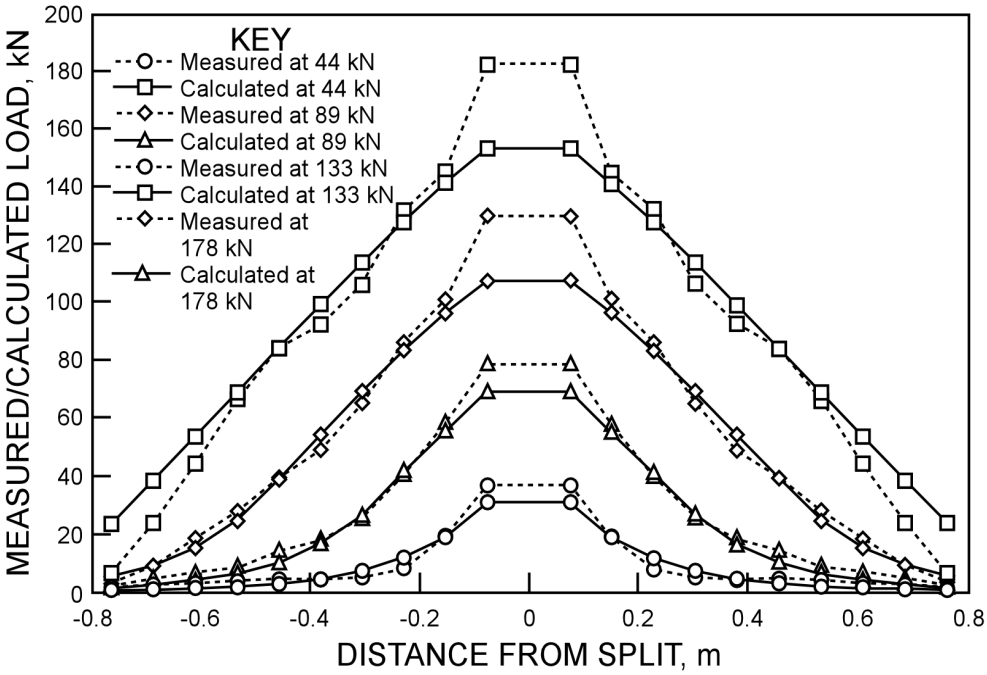

Figure 15.—Plot of laboratory loads and model cable loads at 44, 89, 133, and 178 kN.

by *FLAC*, and the difference becomes more significant as load increases. The difference is explained by realizing that the modeled grout remains perfectly intact for the duration of the simulation. In the laboratory, the grout deteriorates at the split as the confinement offered by the other pipe is removed. This can not be simulated by *FLAC*. The reader is reminded that the load at the split is necessarily equal to the applied load and that this is not reflected in the data set because there is not an element included in the model exactly at the split.

CONCLUSIONS

In this investigation, a laboratory split-pipe test on the SRL instrumented cable bolt was modeled using the continuum code *FLAC*. Laboratory boundary conditions were reproduced, and model cable loads were compared to laboratory-measured cable loads for a range of model grout properties. The cable properties were kept constant for the calibration, since these are generally well known.

The important conclusion from this analysis is that the model parameters were determined based on engineering principles and published data, independent of the laboratory results. Although the *FLAC* cable element is simple, the model results indicate very good agreement with the independently determined SRL cable loads. The most significant discrepancy between the two tests was at the 7.6-cm sensor where model cable loads were consistently lower than the laboratory cable loads. The difference between results is either because the grout quality in the model was not reproduced at the split, or because the model grout did not reproduce failure and deterioration at the split due to cable pull-out. The analysis presented above does not test how *FLAC* accounts for the effect of confinement since appropriate data were not available.

It was found that the best agreement between the model and the laboratory experiment was obtained with a grout stiffness (**kbond**) of 1e8 N/m/m and a maximum shear strength (**sbond**) of 200 kN/m.

REFERENCES

CHEKIRED, M., BENMOKRANE, B. and MITRI, H.S. 1997. CTMD: A new cable tension measuring device. Presentation at 99th CIM conference, Vancouver, BC, April 27-30, 1997. Paper WAM2-E1.

CHOQUET, P., and MILLER, F. 1987. Development and field testing of a tension measuring gauge for cable bolts used as ground

support. Presentation at 89th CIM conference, Toronto, ON, May 3-7, 1987. Paper 43, 19 pp.

GORIS, J.M., BRADY, T. M., and MARTIN, L.A. 1993. Field evaluation of cable bolt supports, Homestake Mine, Lead, SD. U.S. Bur. of Mines Report of Investigations 9474, 28 pp.

GORIS, J.M., and CONWAY J.P. 1987. Grouted flexible tendons and scaling investigations. Paper in Improvement of Mine Productivity and Overall Economy by Modern Technology, 13th World Mining Congress, Stockholm, Sweden. Balkema, v. 2, pp. 783-792.

HUTCHINSON, J.D., and DIEDERICHS, M. 1996. Cablebolting in underground mines. Bitech Publishers, Ltd., Richmond, BC.

HYETT, A.J., and BAWDEN, W.F. 1997. Development of a new instrumented cable bolt to monitor ground support loads in underground excavations. Presentation at 99th CIM conference, Vancouver, BC, April 27-30, 1997. Paper WAM2-E3.

ITASCA CONSULTING GROUP, INC., Minneapolis, MN. 2000. FLAC (Fast Lagrangian Analysis of Continua), Version 4.0.

RUEST, M. 1998. Back analysis of instrumented hanging wall cable bolt reinforcement at Complexe Bousquet. M.Sc. (Eng.) thesis, Queen's University.